

WIRELESS, MAGNET-BASED EYE TRACKING IN LAB ANIMALS

A Design Project Report

Presented to the School of Electrical and Computer Engineering
of Cornell University

in Partial Fulfillment of the Requirements for the Degree of
Master of Engineering, Electrical and Computer Engineering

Submitted by

Thomas Lin, Jialin Song

MEng Field Advisor: Professor Hunter Adams

MEng Outside Advisor: Professor Madineh Sedigh-Sarvestani

Degree Date: May, 2026

Abstract

Master of Engineering Program
School of Electrical and Computer Engineering
Cornell University
Design Project Report

Project Title: Wireless, Magnet-Based Eye Tracking in Lab Animals

Authors: Thomas Lin, Jialin Song

Abstract: Some biology experiments require eye-tracking for small, active animals. This is conventionally accomplished by way of head-mounted cameras, but these camera-based systems are bulky and require a lot of energy. The bulkiness affects the animal's motion, and the energy inefficiency limits the length of an experiment to the battery-life of the device. This project validates a magnet-based alternative: tracking eye movements using a small magnet implanted on the eye and a head-mounted magnetic sensor. Using a physical eye simulator and a Raspberry Pi Pico data acquisition system, we compared two architectures at 100 Hz. The digital 3-axis TMAG5170 sensor has high noise (up to 10° peak-to-peak jitter), requiring aggressive filtering that destroys temporal resolution. Conversely, the analog AMR TMAG6180 sensor has significantly lower noise (only about 1° peak-to-peak jitter). We conclude the analog AMR sensor is better to provide a reliable foundation for future 3D eye-tracking systems.

Individual Contributions

Thomas Lin: Embedded C code, Python script, PCB design, final report draft

Jialin Song: Circuit soldering, bracket & ping-pong ball setup, poster draft

Executive Summary

The goal of this project is to build a hardware prototype to investigate the feasibility of a wireless, magnet-based eye-tracking system for lab animals. Current video-based systems are bulky, energetic, and require high data bandwidth. By implanting a small magnet on the eye and attaching a magnetic sensor to the head, we aim to develop a lightweight, low-bandwidth alternative.

To determine the optimal sensor, we built a physical eye simulator and compared two sensors: the TMAG5170 3-axis linear Hall-effect sensor and the TMAG6180 analog AMR angle sensor, using a Raspberry Pi Pico for data acquisition. During hardware assembly, we discovered that hand-soldering the sensors' tiny 0.65 mm pitch packages was highly unreliable and prone to shorting, leading us to design custom PCBs.

Through 100 Hz high-frequency testing, we found that the digital TMAG5170 sensor has large noise (up to 10° of peak-to-peak jitter and 2.03° of RMS noise). Conversely, the TMAG6180 analog sensor has much lower noise, with only 1° of peak-to-peak jitter and 0.27° of RMS noise.

Ultimately, we validated the magnet-based tracking concept and concluded that the TMAG6180 analog AMR sensor is better for this application. Future work will require multi-sensor arrays and mathematical models to track full 3D eye orientation.

1. Introduction and Problem Statement

Precise eye tracking is fundamental to visual neuroscience, providing critical insights into attention and decision-making. However, while eye tracking is simple in constrained subjects, monitoring eye movements in small, freely moving animals remains a significant engineering challenge.

The state-of-the-art solution, video-oculography (Figure 1), relies on bulky cameras.^[1] These systems are uncomfortable for the animal and require high data bandwidth, making them unsuitable for wireless, unconstrained experiments.

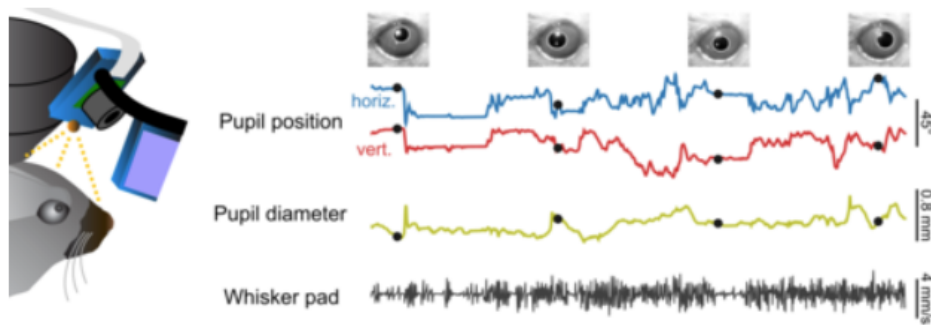


Figure 1: Current video-camera based approach for eye-tracking^[1]

To address these issues, a magnet-based eye-tracking system is proposed: implanting a small magnet on the surface of the eye and attaching a magnetic sensor to the head (Figure 2). As the eye moves, the magnetic sensor detects changes in the magnetic field to calculate the current orientation of the eye.

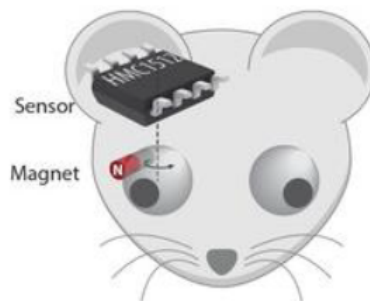


Figure 2: Magnet-based approach for eye-tracking^[2]

The purpose of this project is to build a prototype and conduct proof-of-concept tests to verify the feasibility of this magnet-based approach.

Main Design Specifications:

- **High-Speed Sampling**
Achieve a 100 Hz sampling rate to adequately capture rapid eye movements.
- **Low Noise**
Maintain a stable angle calculation with minimal degrees of jitter or error.
- **Miniaturization Potential**
The whole system should eventually be attached to the lab animal's head.

2. System Options and Selected Approach

We began by evaluating magnetic sensors suitable for our application. While there is a wide range of linear Hall-effect sensors that can measure magnetic field intensity along a single direction, our goal is to calculate the precise orientation of the magnet on the eye. Therefore, we needed a sensor capable of measuring the multi-dimensional angle of the magnetic field. This requirement narrowed our options down to two choices: a 3-axis linear Hall-effect sensor and an analog AMR angle sensor. To determine the optimal solution, we selected the Texas Instruments TMAG5170 3-axis linear Hall-effect sensor and the Texas Instruments TMAG6180 analog AMR angle sensor for comparative testing.

The Texas Instruments TMAG5170 3-axis linear Hall-effect sensor (Figure 3) features integrated X, Y, and Z Hall elements on the chip, enabling it to measure magnetic field intensity along all three axes simultaneously.^[3] It communicates via SPI interface.

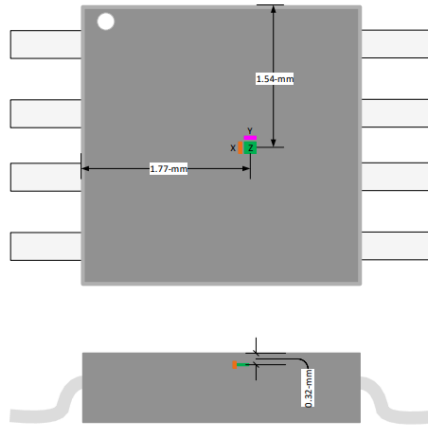


Figure 3: TMAG5170 3-axis linear Hall-effect sensor^[3]

The Texas Instruments TMAG6180 analog AMR angle sensor (Figure 4) utilizes anisotropic magnetoresistance (AMR) technology to directly measure the angle of the magnetic field on the XY plane.^[4] This sensor outputs analog voltages corresponding to the sine and cosine values of the detected angle.

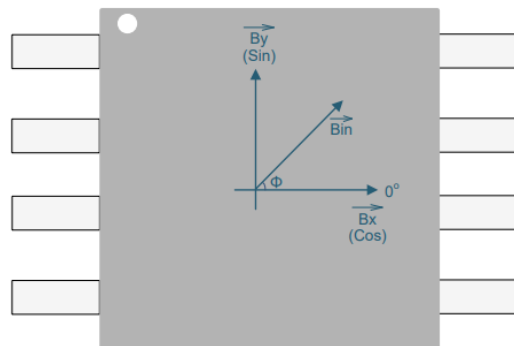


Figure 4: TMAG6180 Analog AMR angle sensor^[4]

We decided to build prototypes with both sensors to further investigate and compare the accuracy and noise characteristics of their angle measurements.

In addition to the magnetic sensors, we use a Raspberry Pi Pico for data acquisition and processing. After receiving the raw data from the sensors, the Raspberry Pi Pico processes the measurements and transmits the data to a host PC via USB for real-time analysis (Figure 5).

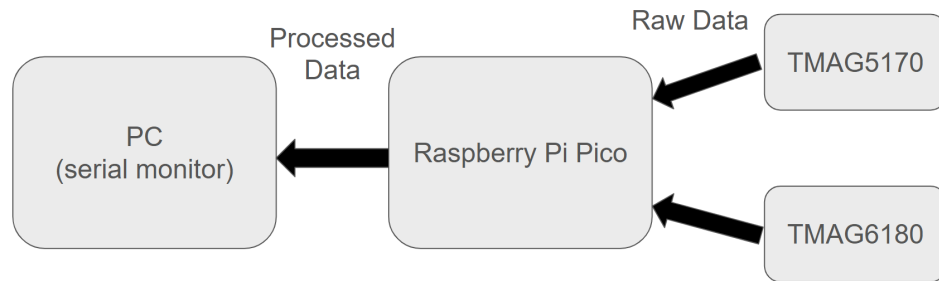


Figure 5: High-level schematic of the prototype

3. Design and Implementation

For the implementation of the prototype, we planned to assemble the circuit on a breadboard. However, the TMAG5170 and TMAG6180 magnetic sensors come in TSSOP-8 packaging with a 0.65 mm pitch, which is incompatible with a standard breadboard (2.54 mm pitch). To connect the sensors to the breadboard, we decided to solder them onto breakout boards to adapt the 0.65 mm pitch to 2.54 mm, and then solder header pins so we could insert the assembly into the breadboard.

This is when we faced our second issue: because the 0.65 mm pitch on the sensor is extremely small, it is nearly impossible to perfectly solder by hand. When we tried to solder the sensors onto the breakout boards, it was very difficult to create a proper connection without accidentally shorting the adjacent pins. Furthermore, there is almost no way to fix the soldering if the pins become shorted, so we ended up discarding several chips and breakout boards.

After considerable effort, we only managed to get one of the sensors soldered correctly (Figure 6). However, the connection was not stable, so we were still unable to get reliable measurements from this implementation.

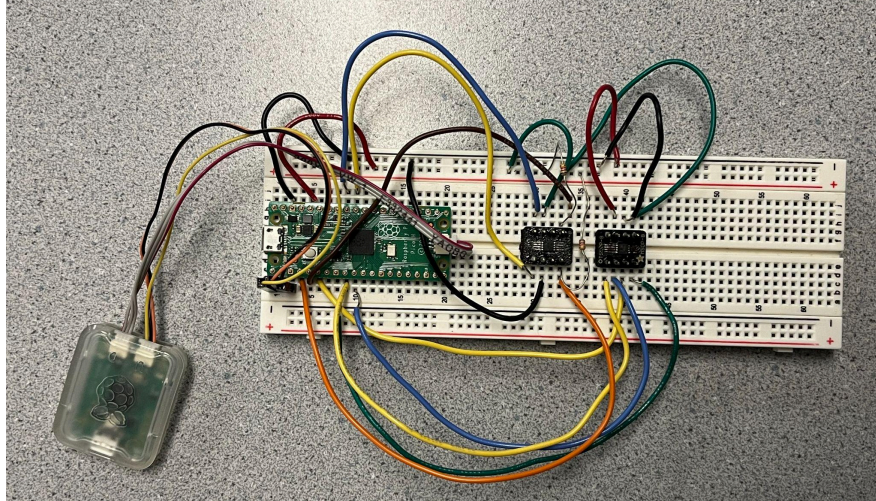


Figure 6: First iteration of the prototype

Since hand-soldering the sensors to the breakout boards is unreliable, our advisor, Professor Hunter Adams, suggested that we order custom PCBs with the sensors factory-assembled on them, so there is no need to solder the tiny pins ourselves.

While designing the PCB, we realized we could also integrate the decoupling capacitors and pull-up resistors specified in the sensor datasheets, so that we would not need to assemble those individual elements on the breadboard.

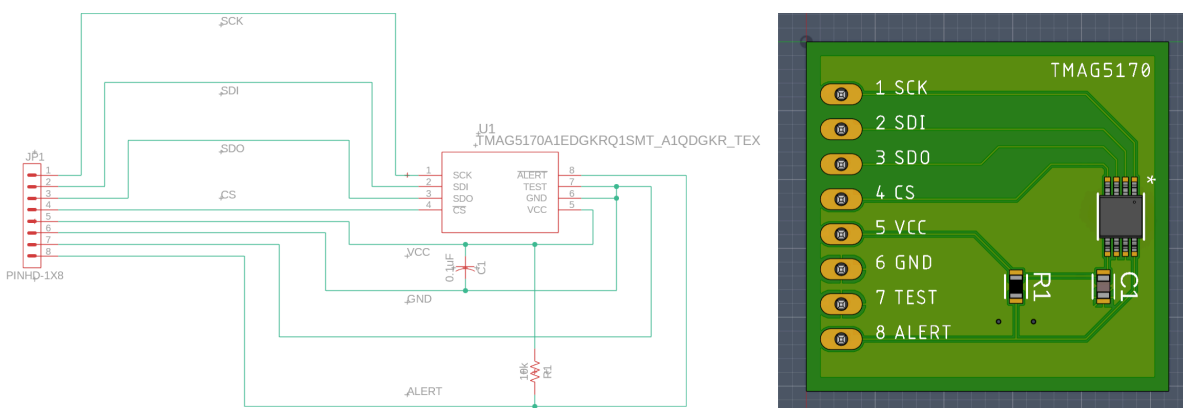


Figure 7: PCB schematic and layout for TMAG5170 3-axis Hall-effect sensor

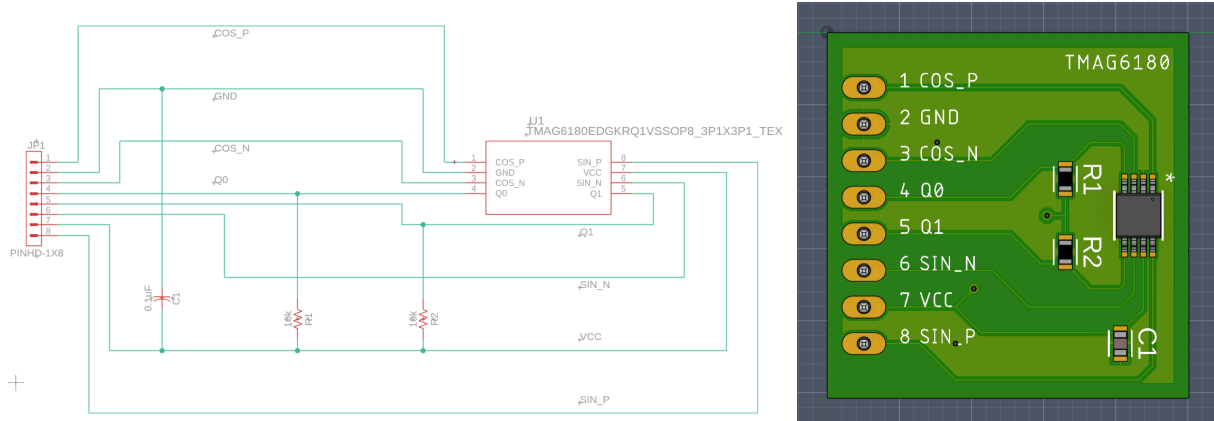


Figure 8: PCB schematic and layout for TMAG6180 analog angle sensor

With the PCBs pre-assembled, we only needed to solder the header pins to insert the boards into the breadboard, and then connect the I/O pins from the Raspberry Pi Pico to the PCBs. This greatly simplified the circuit assembly, making the hardware much more robust and ensuring better wire connections.

Apart from the circuit hardware, we also needed a mechanical device to simulate the eye-magnet system. We attached a magnet to a ping-pong ball and built a simple bracket to hold it in place. By marking angles on the bracket, we established a physical ground-truth angle for the magnet to compare against the measured angles from both sensors.

Although the ultimate goal of this project is to measure 3D eye orientation, we started by simplifying the problem and restricting the magnet's rotation strictly to the Z-axis. The device is set up as follows: the sensor is placed on the XY plane, and the bracket holds the ping-pong ball directly above the sensor. The ping-pong ball only rotates along the Z-axis (Figure 9). Note that the magnet is attached to the bottom side of the ping-pong ball (not visible in the picture). Since the ping-pong ball must be directly above the sensor during measurement, we move the bracket back and forth between the two sensor boards when collecting data for each.

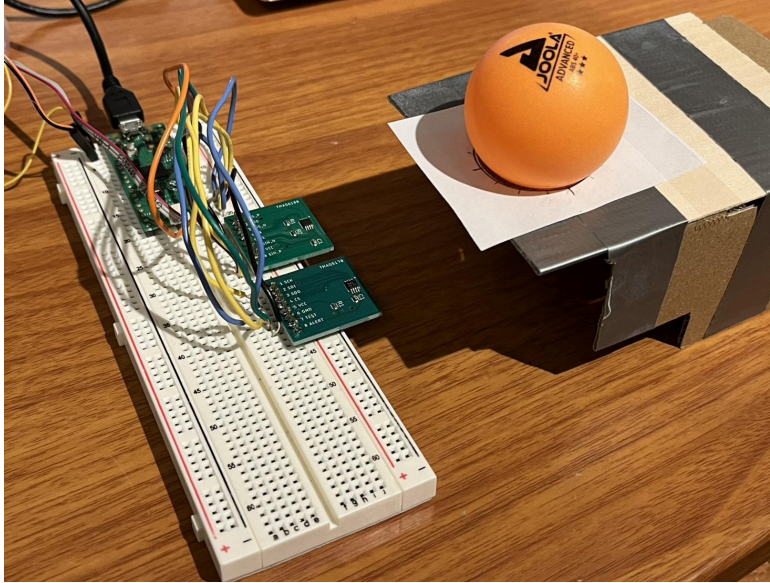


Figure 9: Hardware setup for measurements

Because the magnet remains directly above and parallel to the sensor during measurement, we can calculate its orientation on the XY plane using the following trigonometric equations:

TMAG5170 (3-Axis Linear Hall-Effect Sensor)

$$\text{angle} = \text{atan2}(-B_y, -B_x) \times \frac{180}{\pi}$$

TMAG6180 (Analog AMR Angle Sensor)

$$\text{angle} = \frac{\text{atan2}(V_{\sin}, V_{\cos})}{2} \times \frac{180}{\pi}$$

Note that the raw angle output of the AMR sensor is twice the value of the actual physical angle of the magnetic field. Consequently, we must divide it by 2, which causes the measurement range of the TMAG6180 to wrap around at 180°.

4. Testing and Verification

Our first test was to determine the accuracy of both sensors. We placed the ping-pong ball model in the measurement bracket and recorded the measured angles against the ground-truth angle in 22.5° increments. We initially ran this test at a sampling rate of 10 Hz. The raw data was processed on the Raspberry Pi Pico to calculate the floating-point angles, and the real-time angle measurements were then transmitted to the PC serial monitor.

During this test, we found that the noise level was too high. With the magnet held at a fixed angle, the displayed angle jittered with a range as high as 10° , which was not practical for recording usable accuracy data.

To achieve a stable angle display for this baseline test, we decided to apply a digital moving-average (low-pass) filter in the firmware. Maintaining the same 10 Hz sampling rate, we averaged the most recent 50 samples, meaning the displayed angle was the rolling average of the past 5 seconds. While this stabilized the output, averaging measured data over a 5-second window is not practical for our final application, as the ultimate goal is to track fast eye movements. If we need to low-pass the signal, we must set a much higher cutoff frequency to retain useful information. Therefore, we needed to further investigate the noise characteristics of the hardware.

This led to our second test: high-frequency noise characterization. In this experiment, we wanted to characterize the noise for both sensors without the heavy low-pass filter to see if it was possible to separate the noise from the useful signal. To properly measure this noise, we increased the sampling rate to 100 Hz, fixed the magnet angle at 45° , and continuously measured for 5 seconds, resulting in 500 samples.

Because the 100 Hz sampling rate required much tighter timing constraints, we wanted to prevent the Raspberry Pi Pico from doing too much onboard calculation (such as floating-point calculations). We optimized the system by configuring the Pico to output only the raw data. We then wrote a Python script on the host PC to

catch the serial data, calculate the trigonometry, and write the final results to a CSV file for frequency spectrum analysis.

5. Results

5.1 Accuracy Tests (10 Hz, Low-Pass Filtered)

Below are the results from the first experiment, utilizing the 5-second moving average to test baseline trigonometric accuracy:

ground-truth angle	TMAG5170		TMAG6180	
	measured angle	error angle	measured angle	error angle
0	3.6	3.6	4.7	4.7
22.5	19.3	-3.2	28.2	5.7
45	52.2	7.2	49.3	4.3
67.5	72.1	4.6	72.7	5.2
90	89.1	-0.9	93.7	3.7
112.5	116.9	4.4	107.1	-5.4
135	136.5	1.5	129	-6
157.5	157.1	-0.4	148	-9.5
180 (0)	174.6	-5.4	0.7	0.7
202.5 (22.5)	202.7	0.2	21.5	-1
225 (45)	221.2	-3.8	46.1	1.1
247.5 (67.5)	242.3	-5.2	67.1	-0.4
270 (90)	271.7	1.7	88.9	-1.1
292.5 (112.5)	303.1	10.6	118.7	6.2
315 (135)	321.1	6.1	141.7	6.7
337.5 (157.5)	345.6	8.1	169	11.5

Table 1: Ground-truth angle vs. measured angle for both sensors

Note that the measurement on the TMAG6180 wraps around when exceeding 180° due to the AMR math calculation. In the ground-truth column, the angles in parentheses are the corresponding ground-truth values for the TMAG6180.

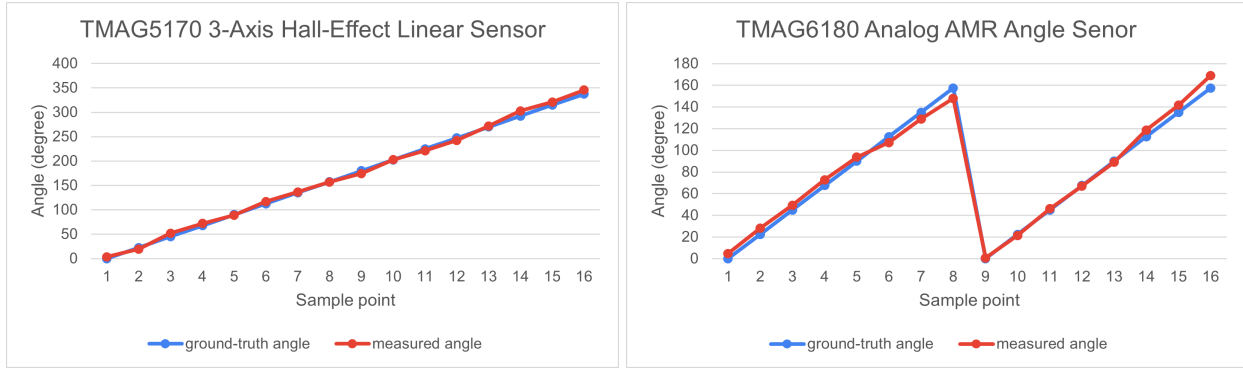


Figure 10: Ground-truth angle vs. measured angle for both sensors

From these results, we observed that after applying the low-pass filter, the error angles for both sensors were generally within 10° . This confirms that both the digital 3-axis and analog AMR calculation methods are fundamentally accurate and could be acceptable for real applications on lab animals, provided the noise can be managed without destroying the temporal resolution.

5.2 Noise Characteristics (100 Hz, Unfiltered)

The following charts shows the raw noise characteristics captured during the 100 Hz high-frequency test:

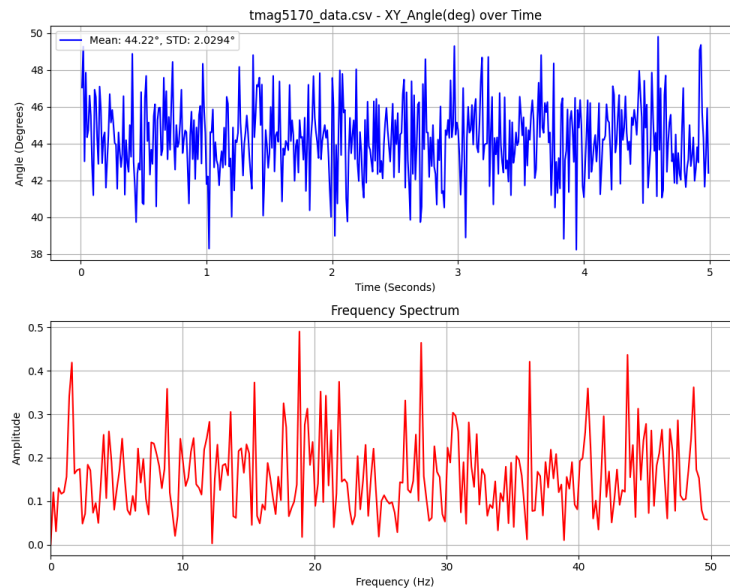


Figure 11: Noise Characteristics for TMAG5170 3-axis Hall-effect sensor

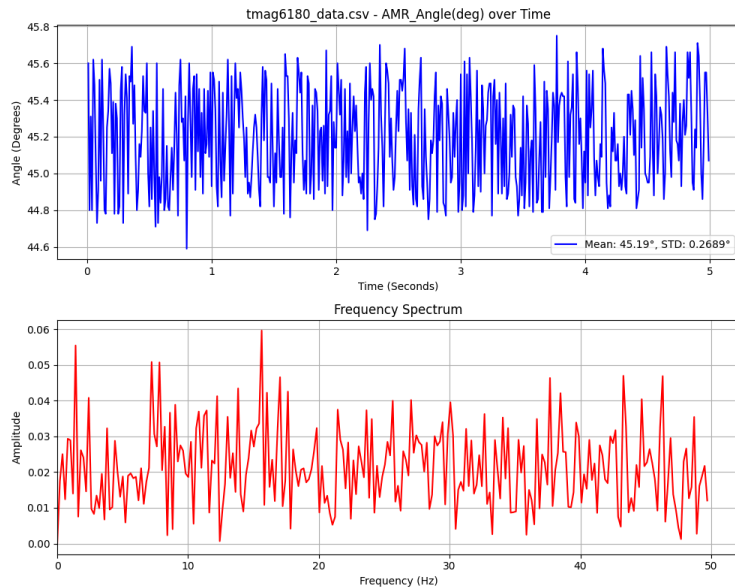


Figure 12: Noise characteristics for TMAG6180 analog AMR angle sensor

As shown in the data, the noise was significantly larger on the TMAG5170 3-axis sensor, with peak-to-peak jitter reaching up to 10° . Conversely, on the TMAG6180 analog angle sensor, the peak-to-peak jitter was only about 1° . The standard deviation (RMS noise) on the TMAG5170 was approximately 2.03° , which is significantly larger than the TMAG6180's 0.27° .

According to the frequency spectrum plots, the noise level across the measurable 0 to 50 Hz range was roughly uniform for both sensors. This means that in a real application on lab animals, it would be challenging to separate the noise from the useful signal simply by filtering out a specific frequency band. However, the data proves that the analog AMR angle sensor possesses inherently low baseline noise. Even with the raw noise unfiltered, the TMAG6180's signal-to-noise ratio could remain high enough to accurately analyze rapid eye movements.

6. Conclusions

In this project, we built a hardware prototype to conduct proof-of-concept experiments for the future implementation of a wireless, magnet-based eye-tracking system. To determine the optimal hardware architecture, we tested and compared two candidate magnetic sensors: the TMAG5170 digital 3-axis linear Hall-effect sensor and the TMAG6180 analog AMR angle sensor.

We ultimately concluded that the digital 3-axis approach (TMAG5170) is not suitable for this specific application. Its inherent high noise (up to 10° of jitter) would require aggressive low-pass filtering, which destroys the temporal resolution needed to track rapid eye movements.

Conversely, the analog AMR approach (TMAG6180) proved highly successful. It showed significantly lower noise (only 1° of jitter), making it the ideal sensor to accurately measure the fast-changing magnetic fields caused by physiological eye movements.

Additionally, from a manufacturing standpoint, we discovered that hand-soldering tiny 0.65 mm pitch TSSOP packages is highly unreliable and prone to short-circuiting. Future iterations of this project must rely on factory-assembled surface-mount PCBs to ensure mechanical and electrical stability.

7. Future Work

In this project, we restricted the rotation of the ping-pong ball strictly to a single axis (the Z-axis). Because of this constraint, the absolute spatial position of the magnet relative to the sensor did not change; only its rotational angle changed. However, in the final intended application on freely moving lab animals, the ultimate goal is to measure full 3D eye orientation.

When an eye rotates along multiple axes (pitch, yaw, and roll), the physical position of the magnet shifts in 3D space. This movement introduces spatial offsets that will cause our current single-sensor trigonometric measurements to become inaccurate.

For future development, we will need to develop mathematical models to account for this positional offset and dynamically compensate for it in the software. Additionally, expanding the hardware to include an array of multiple magnetic sensors distributed around the eye will likely be necessary to accurately capture and reconstruct true 3D eye orientation.

8. References

- [1] [Meyer, Arne F et al. “A Head-Mounted Camera System Integrates Detailed Behavioral Monitoring with Multichannel Electrophysiology in Freely Moving Mice.” Neuron vol. 100,1 \(2018\): 46-60.e7. doi:10.1016/j.neuron.2018.09.020](#)
- [2] [Hannah L Payne, Jennifer L Raymond \(2017\) Magnetic eye tracking in mice eLife 6:e29222](#)
- [3] [Texas Instruments TMAG5170 High-Precision 3D Linear Hall-Effect Sensor datasheet](#)
- [4] [Texas Instruments TMAG6180-Q1 Automotive High-Precision Analog AMR Angle Sensor datasheet](#)
- [5] [Raspberry Pi RP2040 datasheet](#)
- [6] [Raspberry Pi Pico datasheet](#)

9. AI Declaration

After writing the first draft of this report, Google Gemini is used to polish the language use, without rewriting the whole sentences or paragraphs.

10. Appendices

Part List

Name	Product Number	Quantity
Raspberry Pi Pico (RP2040)	SC0917	1
High-Precision 3D Linear Hall-Effect Sensor With SPI	TMAG5170	4
Automotive High-Precision Analog AMR 360° Angle Sensor	TMAG6180-Q1	8
SMT Breakout PCB for SOIC-8, MSOP-8 or TSSOP8	1528-1071-ND (Digikey part number)	12
PCB Prototype (TMAG5170 breakout board v1)	-	5
PCB Prototype (TMAG5170 breakout board v2)	-	5
PCB Prototype (TMAG6180 breakout board v1)	-	5
PCB Prototype (TMAG6180 breakout board v2)	-	5

[Project Repository](#): The embedded C code, Python script, and the CSV files of the measured data.

[PCB Gerber Files](#): All the gerber files of the PCB design.